

## Research Article

# Measurement of Coherence Bandwidth in UHF Radio Channels for Narrowband Networks

**Jaroslav Sadowski**

*Faculty of Electronics, Telecommunications and Informatics, Gdańsk University of Technology, Narutowicza 11/12, 80-233 Gdansk, Poland*

Correspondence should be addressed to Jaroslav Sadowski; [jaroslav.sadowski@eti.pg.gda.pl](mailto:jaroslav.sadowski@eti.pg.gda.pl)

Received 31 January 2015; Revised 21 April 2015; Accepted 21 April 2015

Academic Editor: Francisco Falcone

Copyright © 2015 Jaroslav Sadowski. This is an open access article distributed under the Creative Commons Attribution License, which permits unrestricted use, distribution, and reproduction in any medium, provided the original work is properly cited.

This paper presents results of investigation on the coherence bandwidth of narrowband radio channels in 430 MHz band. The coherence bandwidth values were estimated from a power delay profile obtained by recording CDMA2000 forward channel signals during real-field measurements in various environments: medium city, flat terrain, and hilly terrain in northern Poland. The results of measurements are compared with characteristic parameters of UHF radio channel models defined for exemplary narrowband digital system from the TETRA standard. In all of the tested environments, the coherence bandwidth values during most of an observation time were much higher than 25 kHz. Therefore, the fading in tested UHF narrowband channels should be classified as flat fading.

## 1. Introduction

The radio wave propagation phenomena may distort transmitted radio signals in several different ways. Reception of signals distorted during propagation via radio channels with variable characteristics often requires application of proper techniques to reduce effect of quality degradation, mostly caused by multipath propagation. There are many different techniques which allows improving quality of reception in digital radio communication receivers. Some of the most widely known are a spatial diversity receivers and an adaptive receivers with equalizers. Performance of different receiver structures in real environment highly depends on time and frequency characteristics of transmitted signals and radio channels. Therefore, it is often crucial to characterize propagation conditions before or during design of radio system to select proper methods of reception, suitable for the expected type of distortion of radio signals which may occur during operation.

Problem of selection of proper methods of radio signals reception occurred in 2014 during designing a TETRA network for one of polish energy grid operators and defining requirements for equipment in TETRA base stations (BS).

Different BS receiver configurations were taken into account, including three-antenna spatial diversity reception and two-antenna reception with adaptive equalizer. The latest method: adaptive equalization allows compensating, to some extent, signal degradation caused by time-dispersive, and/or frequency selective channels [1]. Although theoretic analysis and even channel models defined in the TETRA standard [2] indicates that in UHF narrowband channels (25 kHz bandwidth) frequency selective fading should not occur, author decided to verify this assumption by measuring UHF radio channels coherence bandwidth in real environments in selected areas of northern Poland. In order to avoid transmitting any radio signals in licensed and crowded frequency band, downlink signals from CDMA2000 base stations were used as channel sounding signals. Although various results of the coherence bandwidth investigations have already been presented in literature [1, 3–5], they either refer to different frequency bands or different environments and therefore should not be used directly in the designing of TETRA networks or similar narrowband systems.

The impact of variable channel parameters such as coherence bandwidth or delay spread on the quality of reception of radio signals depends on modulation scheme and to

some extent also on the receiver structure. For example, in narrowband digital systems, which uses single carrier modulation, large delay spread generated by multipath propagation causes intersymbol interferences which decreases quality of reception. But in case of CDMA signals, large delay spread is advantageous because it simplifies separation of multipath components in RAKE receiver therefore improving path diversity. For the purposes of this paper, the author assumed that because of motivation described above and some limitation of measurement method presented in Section 3 the goal is to verify coherence bandwidth parameters for narrowband systems which cannot take advantage of multipath phenomenon. Therefore, all conclusions were drawn with assumption that lower values of coherence bandwidth and larger delay spread characterizes worse conditions of reception of narrowband signals. It also means that all ambiguities in definitions of parameters presented in Section 2 were resolved to get results representing worst-case scenario (largest delay spread).

## 2. Coherence Bandwidth

The frequency-domain characteristics of the small scale fading which affects radio signals in the multipath propagation channels strongly depends on the ratio between the bandwidth of transmitted signals and a parameter called coherence bandwidth. The coherence bandwidth is the statistical measure of the frequency range over which the channel is considered to be flat, which means that signals with frequencies in the range of coherence bandwidth will most likely experience correlated amplitude fading [1, 6]. Therefore, a wideband signal which occupies frequency band greater than coherence bandwidth will experience frequency selective fading, so the knowledge of the coherence bandwidth of radio channels in the area covered by radio communication system service allows to decide whether the usage of equalizer unit in radio receiver will be advantageous or not.

The coherence bandwidth value is usually understood as frequency separation for which the amplitude (envelope) correlation factor drops to some threshold value, typically 0.5. Direct evaluation of the coherence bandwidth from the definition given in [6, 7] is usually impractical and often not possible, for example, when the measurement method does not allow to separate signal's components in frequency domain. That is why in practice the coherence bandwidth  $B_c$  is usually evaluated from a power delay profile (PDP) and even in some publications ([1, 8]) the description of the coherence bandwidth is limited only to the calculation of  $B_c$  from PDP parameters in time or frequency domain. The power delay profile is a measure of power of signal received through a multipath channel as a function of time delay [1, 9]. It allows to estimate PDP by taking the time and/or spatial average of a squared impulse responses of tested radio channel [1, 6]:

$$P(\tau) = \frac{1}{N} \sum_{i=1}^N |h(t_i, \tau)|^2. \quad (1)$$

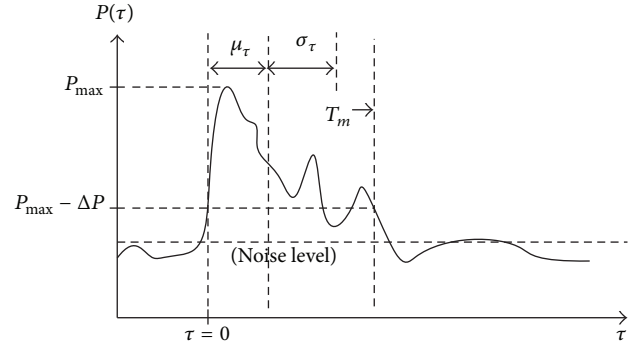


FIGURE 1: Power delay profile and its characteristic parameters in time domain.

Several different parameters are used to characterize power delay profile in time domain. Maximum excess delay  $T_m$  is a time after which the value of  $P(\tau)$  is lower than maximal value by a specified factor  $\Delta P$  (Figure 1). A mean excess delay  $\mu_\tau$  is the first moment of power delay profile defined as

$$\mu_\tau = \frac{\int_{\tau=0}^{T_m} \tau \cdot P(\tau) d\tau}{\int_{\tau=0}^{T_m} P(\tau) d\tau} \quad (2)$$

and a rms delay spread  $\sigma_\tau$  is a square root of the second central moment of PDP:

$$\sigma_\tau = \sqrt{\frac{\int_{\tau=0}^{T_m} (\tau - \mu_\tau)^2 \cdot P(\tau) d\tau}{\int_{\tau=0}^{T_m} P(\tau) d\tau}}. \quad (3)$$

It is commonly known that when some additional conditions are satisfied (propagation characteristics of the channel are random and wide sense stationary, propagation loss, and time delays of multipath components are uncorrelated) all of the time parameters mentioned above are in most cases inversely related to the value of coherence bandwidth  $B_c$ . Unfortunately there is no global agreement on the exact form of such relations. In many publications a simple relation between  $B_c$  and rms delay spread  $\sigma_\tau$  can be found [1, 8–10]:

$$B_{c50} \approx \frac{1}{5 \cdot \sigma_\tau} \quad (4)$$

which is valid for a correlation coefficient equal to 0.5. In case when the threshold correlation value is set to 0.9, approximate equation for the coherence bandwidth value is as follows:

$$B_{c90} \approx \frac{1}{50 \cdot \sigma_\tau}. \quad (5)$$

However, in [3, 11, 12] the authors included a list of alternative forms of formula (4) presented in various publications. In general, the relation between  $B_{c50}$  and rms delay spread may be written as

$$B_{c50} \approx \frac{1}{\alpha \cdot \sigma_\tau}, \quad (6)$$

where coefficient  $\alpha$  takes different values: 1, 5,  $2\pi$ ,  $1/0.15$  and sometimes expression (6) is also written as inequality [13]. For a simple two-ray channel model,  $\alpha$  was found to be equal 6 [14]. In case of an indoor propagation, values of  $\alpha$  may vary from 0.5 to 7 [4]. Some authors also proposed calculation of the coherence bandwidth from  $\sigma_\tau$  taken into noninteger power [15] but in that case the value of an exponent is highly environment-dependent. The formulas for calculation of  $B_c$  from the mean excess value are less frequently presented in literature [7]:

$$B_{c50} \approx \frac{1}{2\pi \cdot \mu_\tau}. \quad (7)$$

Also the approximate equation for calculation of the coherence bandwidth for correlation level 0.9 (5) is usually not discussed in detail in literature.

The value of coherence bandwidth may also be evaluated from power delay profile by calculating its Fourier transform [6, 9, 14, 16]:

$$|S(\Delta f)| = |F(P(\tau))| = \left| \int_{-\infty}^{+\infty} P(\tau) e^{-j2\pi\Delta f\tau} d\tau \right| \quad (8)$$

which is an estimate of the frequency correlation function. Also in this case there is some kind of ambiguity in publications describing problem of coherence bandwidth evaluation: in some of them  $B_{c50}^{FT}$  (values estimated from Fourier transform of PDP will be marked with superscript "FT") is equal to the value of  $\Delta f$ , at which the following condition is met [13]:

$$|S(\Delta f = B_{c50}^{FT})| = 0.5 \cdot |S(\Delta f = 0)| \quad (9)$$

or to twice higher value [1].

Due to fact that different approximate expressions for the coherence bandwidth estimation, mentioned above, are not equivalent, author decided to compare results of  $B_c$  estimation on the basis of the rms delay spread using formulas (4) and (5) for correlation factor 0.5 and 0.9 respectively together with  $B_{c50}^{FT}$  and  $B_{c90}^{FT}$  read from the Fourier transform of the PDP using (9), also for two values of correlation threshold.

Estimation of the coherence bandwidth from the Fourier transform of the power delay profile needs some additional explanation. For some profiles, for example, those with two clearly resolvable peaks which differs in power by several decibels,  $S(\Delta f)$  chart may cross predefined threshold value (typically 50% or 90% of maximal value) more than once (Figure 2). For the purposes of this analysis the author assumed that in such case the coherence bandwidth value will be equal to the lowest frequency  $\Delta f$  at which the chart crosses the threshold value. It may cause some subset of the coherence bandwidth results to be understated, but it does not affect final conclusions on the characteristics of fading in TETRA UHF channels presented in Section 5 of this paper due to fact that even such understated values of coherence bandwidth are greater than bandwidth of narrow-band TETRA channels (25 kHz). However, characterization of fading in wider channels, for example, several hundreds

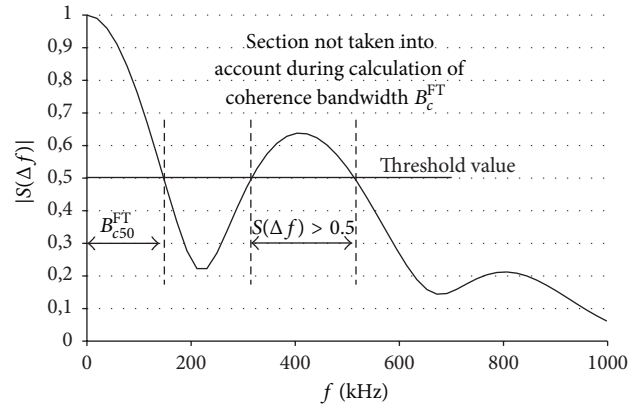


FIGURE 2: Evaluation of coherence bandwidth from Fourier transform of power delay profile in case when  $S(\Delta f)$  crosses predefined threshold value several times.

of kHz (which is not a part of this article) on the basis of measurement results presented in Section 5 must take into account that the assumption mentioned above may change the proportion between flat fading and frequency-selective fading conditions.

### 3. Method of Measurements

The TETRA trunking network for power grid operators in Poland is planned to work in frequency band 416/426 MHz. In order to avoid transmitting test signals in this licensed part of UHF band, the forward (downlink) signals from existing CDMA2000 base stations were selected to act as the channel sounding signals. Therefore, this method of measurements is a modification of sliding correlator method [17, 18] also called correlative sounder [13] which utilize existing radio signals from cellular network. One of the polish CDMA2000 networks uses downlink frequency 424 MHz which is very close to the TETRA band. This network was optimized to achieve high coverage instead of high capacity; therefore, the cell radii are usually quite large. Low density of base stations with antennas mounted relatively high makes propagation condition in this CDMA2000 network similar to those in typical TETRA networks. Therefore, results of the PDP and coherence bandwidth estimation based on CDMA forward signals should be in agreement with parameters of radio channels for TETRA in the UHF band.

It should be noted that using the CDMA2000 forward channel signals for coherence bandwidth estimation has some disadvantages. Firstly, limited bandwidth of the transmitted signals (1.25 MHz) together with limited bandwidth of reception (see description of receiver used for signals recording in Section 3.1) significantly influences lowest measured values of rms delay spread. It is caused by the fact that the channel response measured at the output of CDMA correlation receiver is a convolution of real channel response and shape of transmitted waveform [3, 19] or in our case: shape of autocorrelation function of transmitted CDMA signals. Defining  $\sigma_{\tau, \text{waveform}}$  as a square root of the second central

TABLE I: Relation between measured and real parameters of radio channel for  $\sigma_{\tau, \text{waveform}} = 0.33 \mu\text{s}$ .

		RMS delay spread [ $\mu\text{s}$ ]								
Real	0.1	0.2	0.3	0.4	0.5	0.6	0.7	0.8	0.9	1
Measured	0.34	0.38	0.44	0.51	0.59	0.68	0.77	0.86	0.95	1.05
		Coherence bandwidth estimated from RMS delay spread [kHz]								
Real	100	200	300	400	500	600	700	800	900	1000
Measured	98	189	268	333	385	426	458	483	502	518

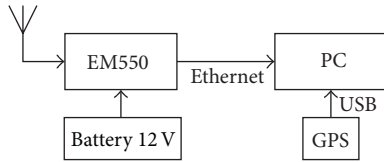


FIGURE 3: Block diagram of mobile measurement set for CDMA-2000 signals recording.

moment of transmitted CDMA waveform autocorrelation function and  $\sigma_{\tau, \text{meas}}$  as value measured using definition in (3), real value of the rms delay spread of radio channel  $\sigma_{\tau, \text{channel}}$  is usually evaluated as [3, 19]:

$$\sigma_{\tau, \text{channel}} = \sqrt{\sigma_{\tau, \text{meas}}^2 - \sigma_{\tau, \text{waveform}}^2} \quad (10)$$

Unfortunately the exact value of  $\sigma_{\tau, \text{waveform}}$  was not known because it was not possible to directly connect source of test signal to the equipment used to record signals from CDMA2000 network. However, approximate value of  $\sigma_{\tau, \text{waveform}}$  may be evaluated from the lowest value of rms delay spread measured in LOS condition in proximity to base station which was  $0.33 \mu\text{s}$  (the same value was measured in all the tested environments presented in Section 3.2). Exemplary values of delay spread correction calculated from (10) and corresponding coherence bandwidth correction for  $\sigma_{\tau, \text{waveform}} = 0.33 \mu\text{s}$  are presented in Table 1. Due to fact that the  $\sigma_{\tau, \text{waveform}}$  value was not verified, this correction of rms delay spread and coherence bandwidth was not applied to the results of measurements presented in Section 5 of this paper.

Second disadvantage of using CDMA2000 signals for channel sounding comes directly from the principles of direct-sequence code division multiple access method. Radio networks which uses this technique are built as single-frequency networks, which means that signals from several neighboring base stations and even from several sectors of the same base station are transmitted in the same channel and are being simultaneously received by mobile terminal so the signal to interference ratio at the output of correlation receiver is significantly degraded by high level of cochannel interferences. To reduce the effect of interferences, only channel impulse responses with main peak greater than 20 dB above interference power level and other multipath components greater than 6 dB above mean interference level were taken into account during power delay profile estimation.

Taking into account disadvantages described above it may be stated that CDMA2000 signals are not a best choice for general radio channel sounding. Dedicated signals made

of wideband pulses or spread-spectrum signal which is not a part of real communication network will surely give more accurate results, but emission of such sounding signals in licensed band in Poland was not possible due to legal restrictions. However, CDMA2000 signals are still sufficient for characterization of fading characteristics in narrowband channels which is a goal of this publication.

**3.1. Measuring Equipment.** The CDMA2000 forward channel signals were recorded for offline processing using equipment presented in Figure 3. This measurement set was mounted in a car with an omnidirectional receiving antenna (gain: 4.5 dBi) mounted on car roof using magnetic base. A general purpose receiver EM550 from Rohde & Schwarz was responsible for all RF processing including I/Q demodulation and signal sampling. Stream of I/Q samples was sent to a PC computer via an Ethernet interface. Dedicated software was performing signal processing tasks presented in form of a block diagram in Figure 4. Due to fact that signals from different base stations and different sectors in the same base station are spread by the same pair of pseudorandom sequences but with different time shift (code phase), the coarse synchronization block was responsible for rough estimation of time of arrival of CDMA signals from different transmitters by finding local maxima of cross correlation function of received signals and locally generated time-shifted short code PN sequences identical to those used in base stations in forward pilot channel (Walsh code number 0) [2]. Although the maximal value of despreading signal may not always indicate the first component in case of the multipath propagation, it does not influence the power delay profile analysis in any way due to estimation of PDP also before time indicated by the coarse synchronization block. After coarse synchronization, all the other tasks presented on block diagram in Figure 4 were performed in parallel for signals from all detected transmitters, with the only difference in time shift of PN sequences.

Besides the forward pilot channel, the only decoded physical channel in CDMA2000 downlink signal was a forward sync channel identified by Walsh code number 32. The forward sync channel is not encrypted and contains a sync message with short code offset index, which may be understood as base station and sector identifier. Correct decoding of the sync message was used as a proof that a valid CDMA2000 signal was found. The most important task was to calculate samples of power delay profile in time span  $\pm 26 \mu\text{s}$  relative to previously found coarse synchronization. PDP samples were estimated by correlation of received

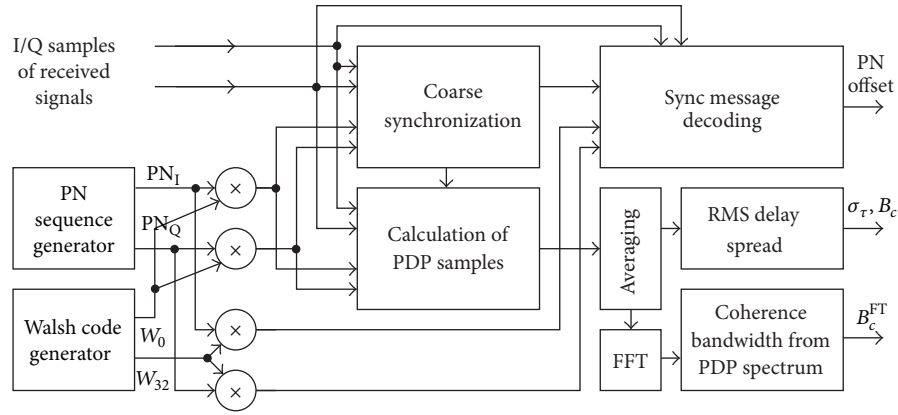


FIGURE 4: Block diagram of signal processing in dedicated PC software.

TABLE 2: Characteristic values of rms delay spread for UHF narrowband channels.

Parameter	City	Hilly terrain	Flat terrain
Median value [ $\mu\text{s}$ ]	0.612	0.46*	0.4*
Value exceeded in 10% of observation time [ $\mu\text{s}$ ]	1.63	1.15	0.49*
Value exceeded in 1% of observation time [ $\mu\text{s}$ ]	4.07	3.09	0.8

\* Values greatly influenced by limitations of PDP measurement method (overestimated).

TABLE 3: Measured values of coherence bandwidth for UHF narrowband channels.

Parameter	City	Hilly terrain	Flat terrain
Number of PDP measurements	64365	59918	169945
Minimal distance to BS [km]	0.46	0.7	12.4
Maximal distance to BS [km]	63.8	81.2	62.7
Coherence bandwidth calculated from rms delay spread for correlation 0.5			
$B_{c50}$ mean value [kHz]	315.4	390.6	479.7
$B_{c50}$ exceeded in 50% of cases [kHz]	318.6	437.3	497.3
$B_{c50}$ exceeded in 90% of cases [kHz]	122.6	173.6	409.8
$B_{c50}$ exceeded in 99% of cases [kHz]	49.1	64.8	248.8
$B_{c50}$ minimal value [kHz]	18	23.4	32.3
$B_{c50}$ below 25 kHz [% of time]	0.1	0.003	—
Coherence bandwidth calculated from PDP Fourier transform for correlation 0.5			
$B_{c50}^{FT}$ mean value [kHz]	392.5	455.4	522.6
$B_{c50}^{FT}$ exceeded in 50% of cases [kHz]	427.4	504.7	534.2
$B_{c50}^{FT}$ exceeded in 90% of cases [kHz]	188.1	272.5	482.3
$B_{c50}^{FT}$ exceeded in 99% of cases [kHz]	75.2	95	356.6
$B_{c50}^{FT}$ minimal value [kHz]	32.4	43.6	48.7
$B_{c50}^{FT}$ below 25 kHz [% of time]	—	—	—
Coherence bandwidth calculated from PDP Fourier transform for correlation 0.9			
$B_{c90}^{FT}$ mean value [kHz]	140.6	167.7	198.6
$B_{c90}^{FT}$ exceeded in 50% of cases [kHz]	145.3	185.9	204.3
$B_{c90}^{FT}$ exceeded in 90% of cases [kHz]	66.8	89.7	176
$B_{c90}^{FT}$ exceeded in 99% of cases [kHz]	36.9	42.8	121.9
$B_{c90}^{FT}$ minimal value [kHz]	21.8	23.5	26.8
$B_{c90}^{FT}$ below 25 kHz [% of time]	0.13	0.013	—

signal with pair of 32768-chip long pseudorandom sequences (short code, 26.7 ms repetition time); therefore, the CDMA processing gain was equal to 45 dB. Finally, the coherence bandwidth values were estimated using two methods with two correlation levels (0.5 and 0.9) from the average of ten consecutive power delay profiles (every 267 ms).

It should be noted that the EM550 receiver is able to send a stream of samples to the external computer via Ethernet interface only when the bandwidth of reception is no wider than 1 MHz, and the sampling rate is limited to 1.28 MHz. Together with limited bandwidth of CDMA2000 (1x) forward signal it strongly limits possibility to estimate the rms delay spread value of radio channel lower than approximately  $0.4 \mu\text{s}$  and the coherence bandwidth wider than approximately 500 kHz (the coherence bandwidth calculated from the rms delay spread for the correlation level 0.5 and calculated from the PDP Fourier transform) or 50 kHz (the coherence bandwidth from the rms delay spread for correlation 0.9). For measurement results which are close to the limits mentioned above, correction based on (10) may be applied to increase their accuracy.

**3.2. Measurement Routes.** The downlink signals from the CDMA2000 base stations were recorded separately in three environments with significantly different radio propagation characteristics:

- (i) City of Gdansk in northern Poland, which is medium-sized (approximately 400 thousand inhabitants) and has various kinds of buildings and land development, will be further called *city*;
- (ii) Region of Gdansk Pomerania located south-west of Gdansk, with relatively large differences in terrain height reaching 200 meters, terrain partially covered by forests and farmlands, will be further called *hilly terrain*;
- (iii) Valley of Vistula river near estuary to Baltic Sea, which is a region with very low variances in height, limited to few meters, mostly covered by farmlands, will be further called *flat terrain*.

These three environments fully cover possible forms of terrain and kinds of land development on the majority of area of Poland. Length of the measurement routes in city and hilly terrain was over 80 km while in flat area exceeded 150 km. During measurements the car was moving with variable speed from 0 to 70 km/h with average 30 km/h in city (duration of measurements: 3 hours) and 45 km/h in other environments (2 and 3.5 hours, resp.).

The CDMA2000 service in almost whole area of Gdansk city is provided by one, centrally located base station with three sectors. However, during measurements performed near city boundaries, signals from eight other base stations located in neighboring cities and surrounding area were also detected and recorded (cochannel signals from single-frequency network, distinguished in CDMA receiver by different time-shift of reference PN sequence during spectrum despread). In the flat and hilly terrain, it was possible to record signals from 11 and 9 base stations, respectively, but in

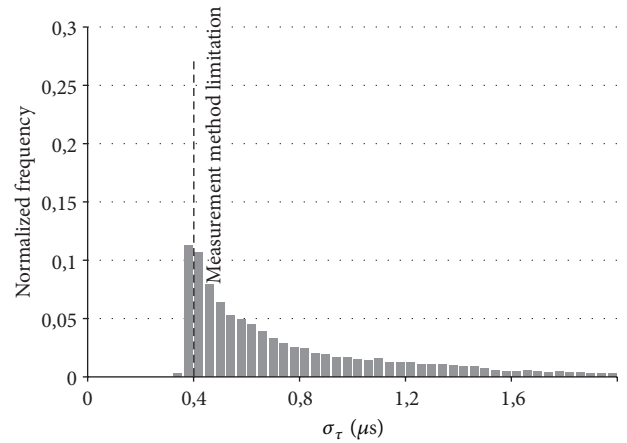


FIGURE 5: Histogram of rms delay spread values measured in city area.

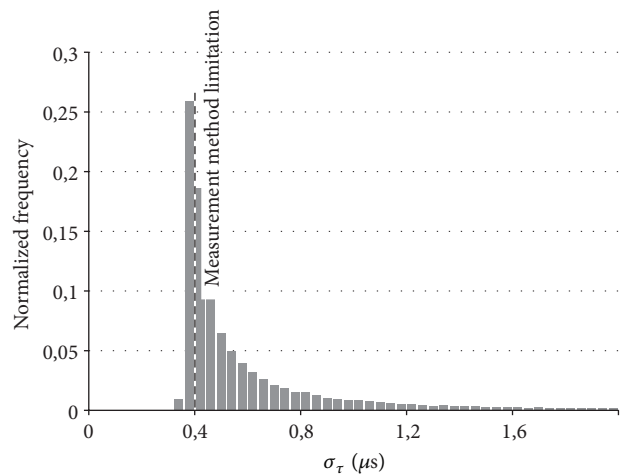


FIGURE 6: Histogram of rms delay spread values measured in hilly terrain.

case of many stations signals from more than one sector were successfully received giving total number of almost 30 unique CDMA2000 transmitters used for channel sounding. The minimal and maximal length of propagation path and total number of power delay profile estimates in all environments are summarized in Table 3.

#### 4. Results of Measurements

Differences in propagation conditions in the three selected environments are clearly visible on rms delay spread histograms presented in Figure 5 (city), Figure 6 (hilly terrain), and Figure 7 (flat terrain) and also on delay spread cumulative distribution chart in Figure 8. During 90% of an observation time the value of rms delay spread estimated from power delay profiles for Gdansk city area was not greater than  $1.63 \mu\text{s}$  and  $1.15 \mu\text{s}$  in hilly terrain and  $0.49 \mu\text{s}$  in flat terrain, although the last value is close to the limitation caused by method of measurements and therefore is overestimated (see Section 3

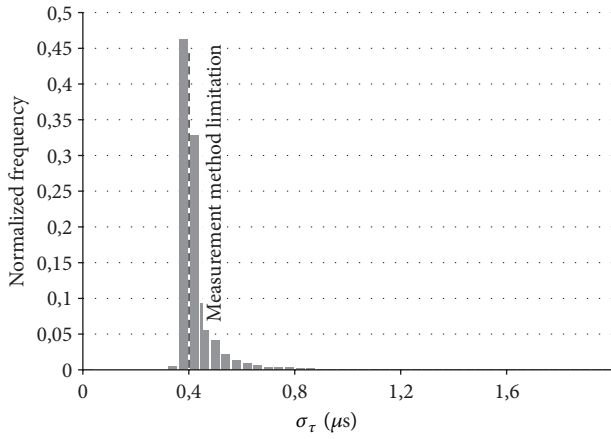


FIGURE 7: Histogram of rms delay spread values measured in flat terrain.

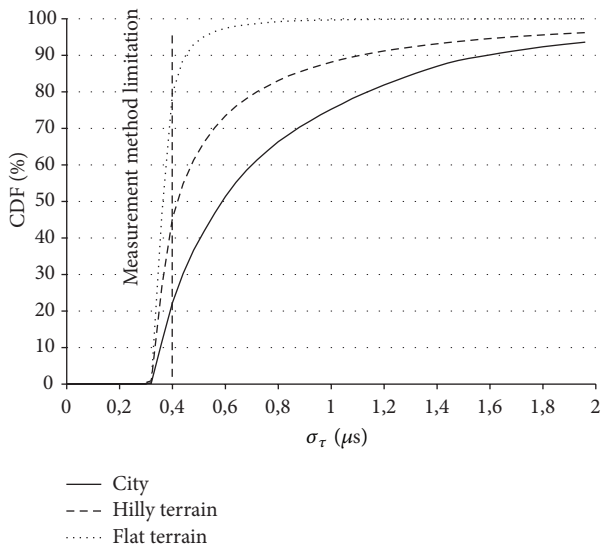


FIGURE 8: Cumulative distribution function of rms delay spread in three environments.

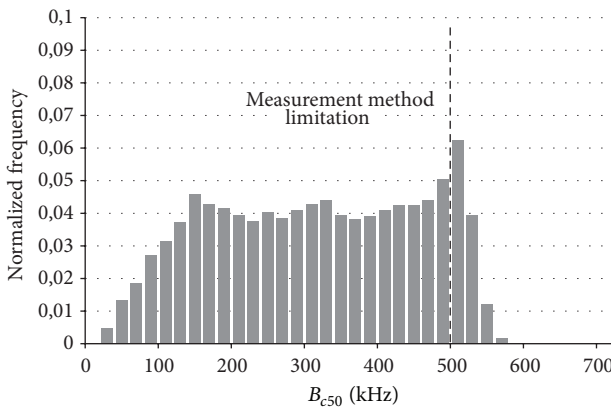


FIGURE 9: Histogram of coherence bandwidth values estimated from rms delay spread for correlation level 0.5 in the Gdansk city area.

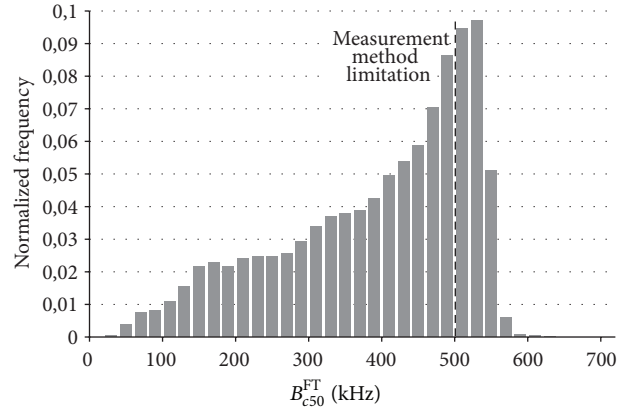


FIGURE 10: Histogram of coherence bandwidth values estimated from Fourier transform of PDP for correlation level 0.5 in the Gdansk city area.

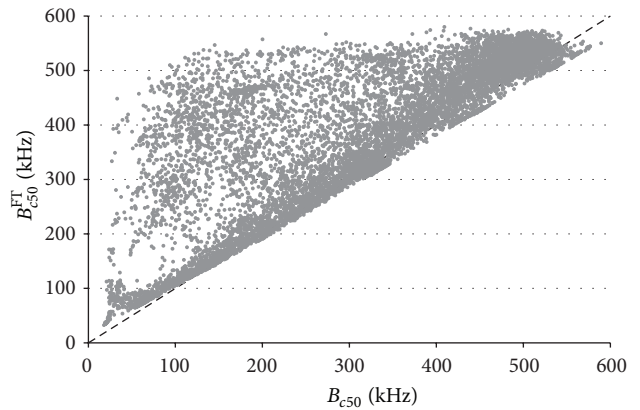


FIGURE 11: Relation between coherence bandwidth estimated from rms delay spread ( $B_{c50}$ ) and from Fourier transform of power delay profile ( $B_{c50}^{FT}$ ) for correlation level 0.5 in the Gdansk city area.

for details). Other characteristic values of measured delay spread are summarized in Table 2.

The histograms of the coherence bandwidth values estimated from the rms delay spread and from Fourier transform of the power delay profile for correlation level 0.5 in Gdansk city area are presented in Figures 9 and 10, respectively. Although these histograms are slightly different, it can be said that the values of coherence bandwidth obtained using both methods are similar. Figure 11 contains dot chart of coherence bandwidth  $B_{c50}^{FT}$  from the PDP Fourier transform (9) as a function of  $B_{c50}$  from the rms delay spread (4). The majority of points in this chart are located near straight line representing equation  $B_{c50} \approx B_{c50}^{FT}$ , which proves that for correlation level 0.5 both methods gives in most cases similar results as for exemplary PDP presented in Figure 12(a). Therefore, the value of coefficient in denominator of (4) seems to be correct for this kind of environment (the same relation was also found for all the other tested environments). However, in some cases the coherence bandwidth estimated from the PDP Fourier transform was up to several times

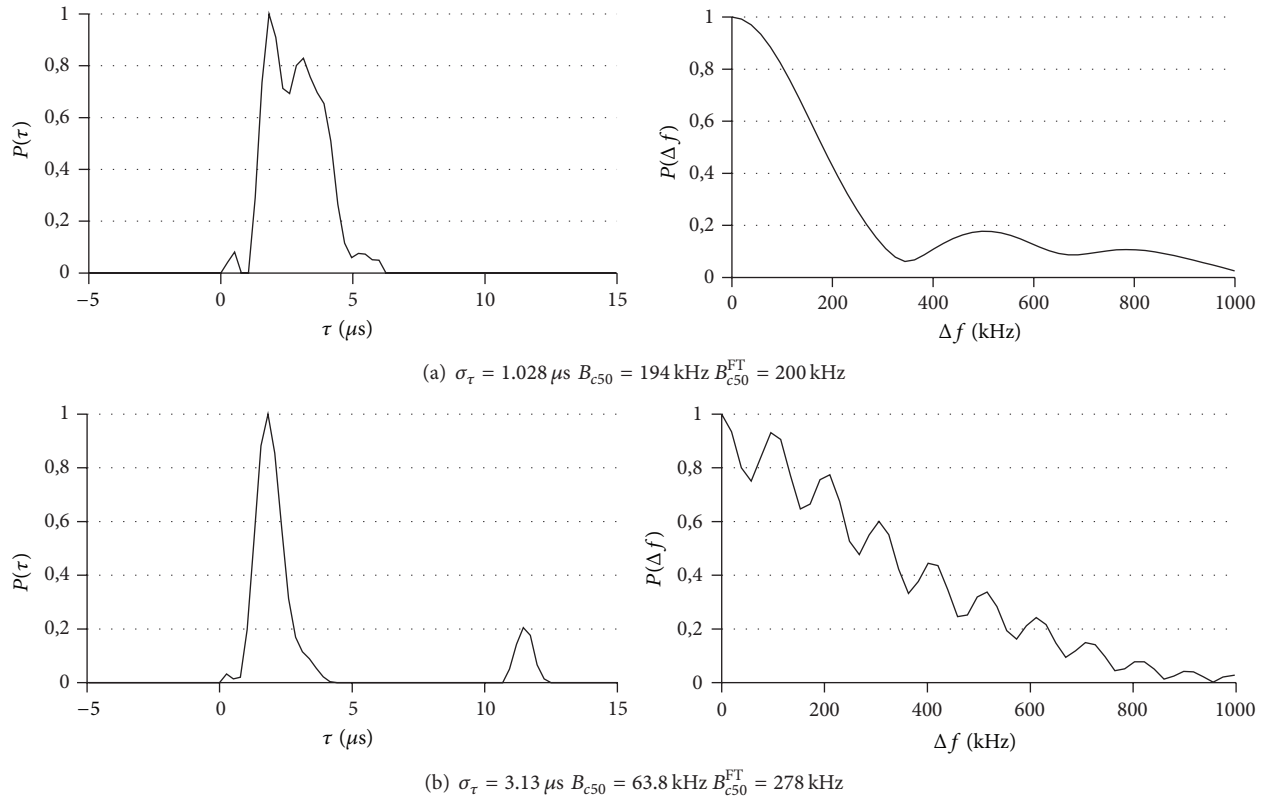


FIGURE 12: Examples of power delay profiles which gives similar (a) and different (b) values of coherence bandwidth.

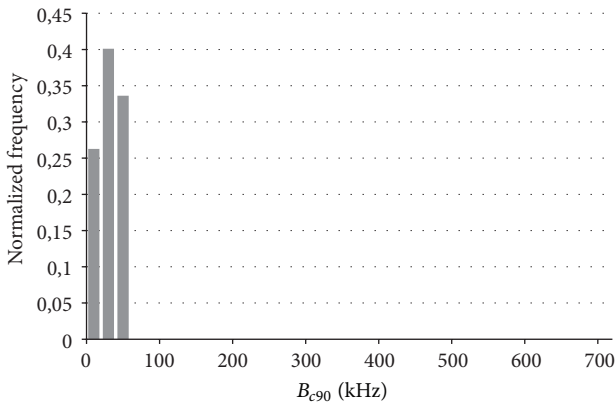


FIGURE 13: Histogram of coherence bandwidth values estimated from rms delay spread for correlation level 0.9 in the Gdansk city area.

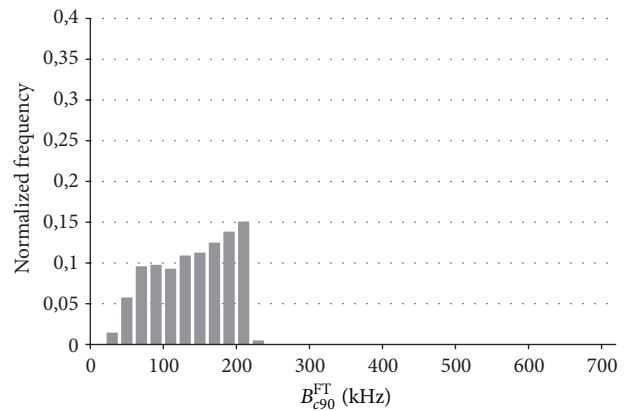


FIGURE 14: Histogram of coherence bandwidth values estimated from Fourier transform of PDP for correlation level 0.9 in the Gdansk city area.

greater than  $B_c$  from the rms delay spread. This happens mostly in case of power delay profiles with two or more peaks with big time separation, as in example presented in Figure 12(b). This effect of big impact of a low power path with large excess delay on the rms delay spread but not on the coherence bandwidth values was also mentioned in discussion on results of channel parameters simulation in [14]. Therefore, it should be taken into account that the coherence bandwidth values estimated from the rms delay spread for correlation level 0.5 may be underestimated for

some power delay profiles and should be understood as a worst case scenario during analysis of channel properties for narrowband systems which cannot take advantage of path diversity.

Although differences in coherence bandwidth for correlation level 0.5 occurred only in some subset of all measurements, results of estimation of  $B_{c90}$  from the rms delay spread (Figure 13) and  $B_{c90}^{\text{FT}}$  from the PDP Fourier transform (Figure 14) for correlation level 0.9 are not even



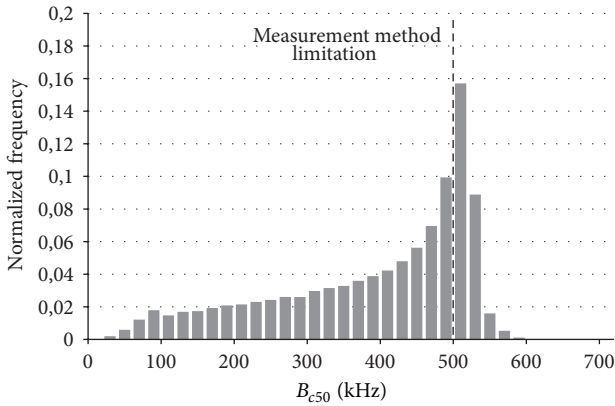


FIGURE 15: Histogram of coherence bandwidth values estimated from rms delay spread for correlation level 0.5 in hilly terrain.

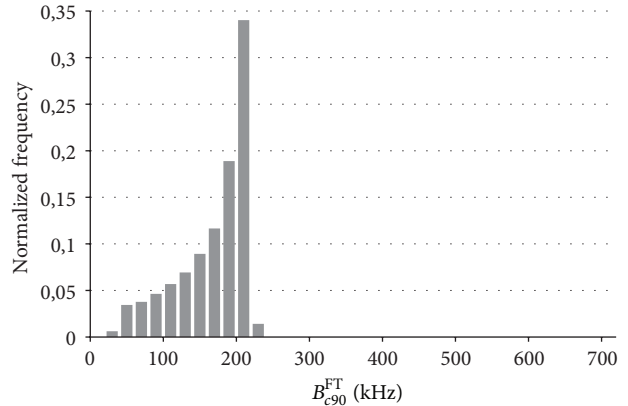


FIGURE 17: Histogram of coherence bandwidth values estimated from Fourier transform of PDP for correlation level 0.9 in hilly terrain.

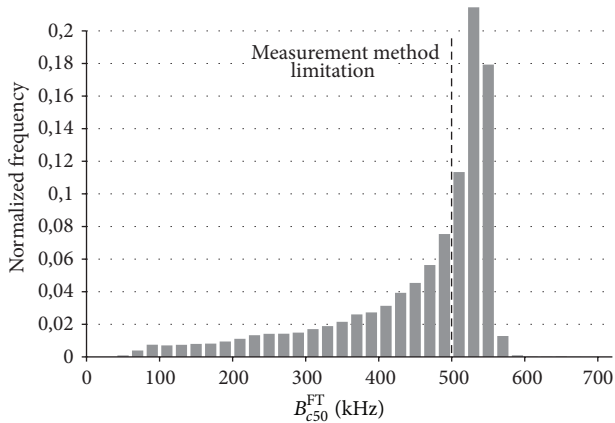


FIGURE 16: Histogram of coherence bandwidth values estimated from Fourier transform of PDP for correlation level 0.5 in hilly terrain.

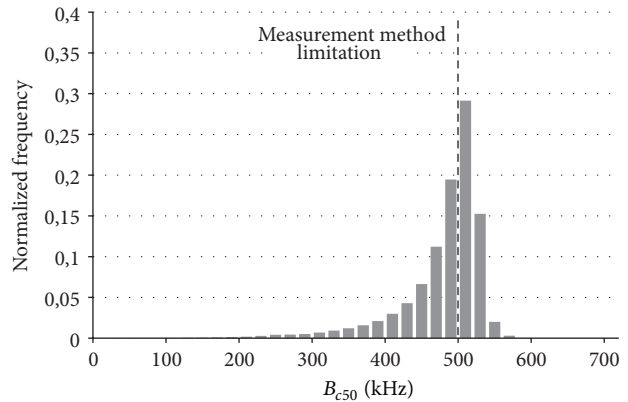


FIGURE 18: Histogram of coherence bandwidth values estimated from rms delay spread for correlation level 0.5 in flat terrain.

similar. All the results calculated from the rms delay spread for correlation level 0.9 are several times lower than the coherence bandwidth from the power delay profile Fourier transform and it seems that (5) should not be used for coherence bandwidth estimation. Therefore, histograms and numerical values of  $B_{c90}$  for other environments (hilly and flat terrain) will not be presented here due to their insufficient reliability.

Figures 15–20 contains histograms of coherence bandwidth values estimated for hilly and flat terrain, respectively, from the rms delay spread for correlation level 0.5 and from Fourier transform of the power delay profile for correlation levels 0.5 and 0.9.

Some characteristic numerical values of coherence bandwidth: mean and median values, values exceeded during 90% and 99% of observation time and minimal observed coherence bandwidth for all specified environments are summarized in Table 3. This table contains also percentage of observation time while the measured coherence bandwidth was below 25 kHz (typical bandwidth of narrowband transmission, e.g., in TETRA).

Please note that also in this table values of  $B_c$  close to 500 kHz are greatly influenced by limitation of measurement method and may be underestimated.

### 5. Conclusion

Analyzing results of the coherence bandwidth investigation presented in Table 3 one can find that the coherence bandwidth values lower than 25 kHz occurred in city area during only 0.1% of observation time (10 seconds in 3 hours of measurements) and even less frequently in hilly terrain (less than one second in 2 hours). Therefore, narrowband transmission systems using 25 kHz wide channels should expect flat fading (propagation through nonfrequency selective channels) in all tested kinds of environments.

To simplify comparison of measured values of the rms delay spread and the coherence bandwidth with multipath propagation models defined in the TETRA standard [2] for signals with DQPSK/D8PSK and QAM modulation in UHF band, time and frequency domain parameters of these models are summarized in Table 4. Comparing data from Tables 2, 3, and 4, it can be stated that in the region of northern Poland

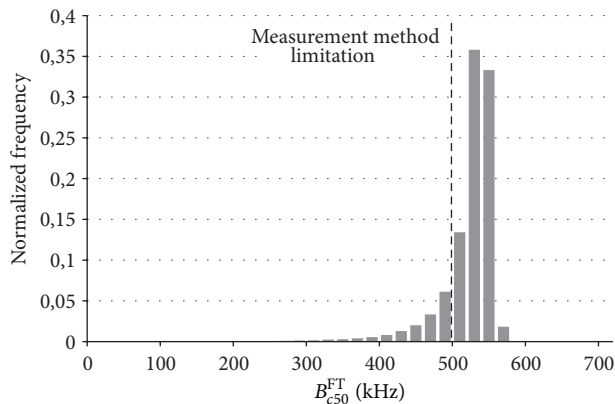


FIGURE 19: Histogram of coherence bandwidth values estimated from Fourier transform of PDP for correlation level 0.5 in flat terrain.

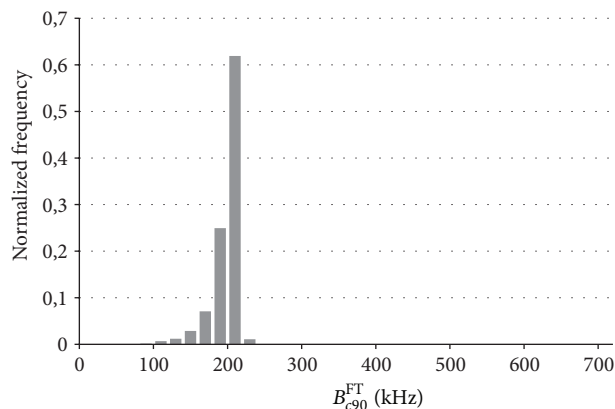


FIGURE 20: Histogram of coherence bandwidth values estimated from Fourier transform of PDP for correlation level 0.9 in flat terrain.

TABLE 4: Coherence bandwidth for channel models defined in TETRA standard.

Channel model	$\sigma_r$ [ $\mu$ s]	$B_{c50}$ [kHz]	$B_{c50}^{FT}$ [kHz]	$B_{c90}^{FT}$ [kHz]
RAx PSK	—	—	—	—
TUx PSK	0.38	524	—	—
BUx PSK	2.36	84.8	84.2	40.5
HTx PSK	4.9	40.8	—	25.2
EQx PSK	17.9	11.1	39.1	17.8
TUx QAM	1.07	187	695	84.5
HTx QAM	5.03	39.7	777	24.7

propagation conditions corresponding to the TETRA models for rural (RAx) and urban (TUx) environments defined for PSK transmission area are most likely to occur. Propagation conditions comparable to bad urban environment (BUx) for DQPSK/D8PSK and urban (TUx) for QAM signals occurred very rare and should be considered as the worst case scenario, not typical conditions.

Taking into account measured values of the coherence bandwidth in selected environments it can be stated that

the TETRA devices working with the DQPSK/D8PSK modes in 25 kHz channels should expect flat fading which cannot be compensated using adaptive equalizers. Also in case of wider channels up to 150 kHz, in which the QAM modulation is used on multiple subcarriers, the adaptive equalizers will not improve quality of reception because the bandwidth of signals transmitted on each subcarrier is much lower than the measured coherence bandwidth of UHF channels even in the worst case scenario [8]. The same conclusions may be applied to other narrowband systems and even to the independent reception of separate subcarriers in multicarrier modulations such as OFDM.

Additional investigation showed no significant relationship between length of propagation path and range of observed coherence bandwidth values.

### Conflict of Interests

The author declares that there is no conflict of interests regarding the publication of this paper.

### Acknowledgments

This work was financially supported by Polish National Centre for Research and Development under Grant No. DOB-BIO6/09/5/2014.

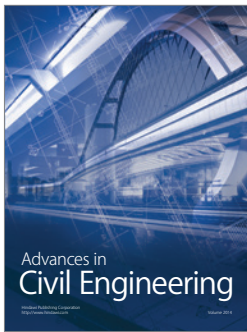
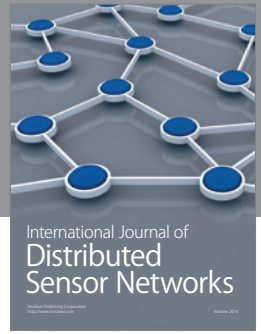
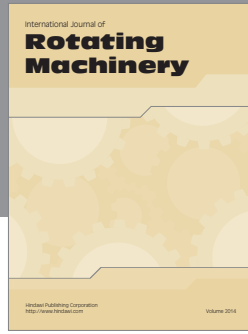
### References

- [1] T. S. Rappaport, *Wireless Communications Principles and Practice*, Prentice Hall, Kindersley, Canada, 2nd edition, 2009.
- [2] Terrestrial Trunked Radio (TETRA), "Voice plus data (V+D); part 2: air interface," ETSI Standard 300 392-2 v3.4.1, ETSI, 2010.
- [3] M. S. Varela and M. G. Sánchez, "RMS delay and coherence bandwidth measurements in indoor radio channels in the UHF band," *IEEE Transactions on Vehicular Technology*, vol. 50, no. 2, pp. 515–525, 2001.
- [4] G. J. M. Janssen, P. A. Stigter, and R. Prasad, "Wideband indoor channel measurements and BER analysis of frequency selective multipath channels at 2.4, 4.75, and 11.5 GHz," *IEEE Transactions on Communications*, vol. 44, no. 10, pp. 1272–1288, 1996.
- [5] M. H. Unar, I. A. Glover, J. Heaton, C. Williams, and P. S. Cannon, "Wide-band mobile radio channel characterisation in UHF band for residential suburban areas," in *Proceedings of the 12th International Conference on Antennas and Propagation*, vol. 1, pp. 262–265, March–April 2003.
- [6] S. Salous, *Radio Propagation Measurement and Channel Modelling*, John Wiley & Sons, 2013.
- [7] M. D. Yacoub, *Foundations of Mobile Radio Engineering*, CRC Press, 1993.
- [8] M. Ergen, *Mobile Broadband Including WiMAX and LTE*, Springer, Berlin, Germany, 2009.
- [9] A. Goldsmith, *Wireless Communications*, Cambridge University Press, Cambridge, UK, 2005.
- [10] J. V. O. Gonçalves and G. L. Siqueira, "Delay spread calculation from coherence bandwidth measurements on a OFDM based mobile communication system," in *Proceedings of the SBMO/IEEE MTT-S International Microwave and Optoelectronics Conference (IMOC '09)*, pp. 253–256, November 2009.



- [11] V. M. Hinostroza, "Frequency selectivity parameters for broadband signals," in *Proceedings of the 7th International Conference on Intelligent Transport Systems Telecommunications (ITST '07)*, pp. 174–179, Sophia Antipolis, France, June 2007.
- [12] F. J. B. Barros, R. D. Vieira, and G. L. Siqueira, "Relationship between delay spread and coherence bandwidth for UWB transmission," in *Proceedings of the SBMO/IEEE MTT-S International Conference on Microwave and Optoelectronic*, pp. 415–420, July 2005.
- [13] A. F. Molisch, *Wireless Communications*, John Wiley & Sons, 2011.
- [14] M. P. Fitton, A. R. Nix, and M. A. Beach, "A comparison of RMS delay spread and coherence bandwidth for characterisation of wideband channels," in *Proceedings of the IEE Colloquium on Propagation Aspects of Future Mobile Systems*, pp. 9/1–9/6, IEEE, London, UK, October 1996.
- [15] K. N. Maliatsos, P. Loulis, M. Chronopoulos, P. Constantinou, P. Dallas, and M. Ikononou, "The power delay profile of the mobile channel for above the sea propagation," in *Proceedings of the IEEE 64th Vehicular Technology Conference (VTC '06)*, pp. 1–5, IEEE, Montreal, Canada, September 2006.
- [16] G. Kalivas, *Digital Radio System Design*, John Wiley & Sons, Chichester, UK, 2009.
- [17] J. Kivinen, T. O. Korhonen, P. Aikio, R. Gruber, P. Vainikainen, and S.-G. Häggman, "Wideband radio channel measurement system at 2 GHz," *IEEE Transactions on Instrumentation and Measurement*, vol. 48, no. 1, pp. 39–44, 1999.
- [18] R. J. Pirkl and G. D. Durgin, "Optimal sliding correlator channel sounder design," *IEEE Transactions on Wireless Communications*, vol. 7, no. 9, pp. 3488–3497, 2008.
- [19] A. A. M. Saleh and R. A. Valenzuela, "A statistical model for indoor multipath propagation," *IEEE Journal on Selected Areas in Communications*, vol. 5, no. 2, pp. 128–137, 1987.





**Hindawi**

Submit your manuscripts at  
<http://www.hindawi.com>

